# Dlg3 Trafficking and Apical Tight Junction Formation Is Regulated by Nedd4 and Nedd4-2 E3 Ubiquitin Ligases

Developmental Cell
Article

# Dlg3 Trafficking and Apical Tight Junction Formation Is Regulated by Nedd4 and Nedd4-2 E3 Ubiquitin Ligases

Claude A. Van Campenhout,[1] Andrea Eitelhuber,[2,8] Christian J. Gloeckner,[4,7,8] Patrizia Giallonardo,[1,8] Moritz Gegg,[1] Heide Oller,[1] Seth G.N. Grant,[5,6] Daniel Krappmann,[2] Marius Ueffing,[4,7] and Heiko Lickert[1,3,*]
[1]Institute of Stem Cell Research
[2]Institute of Toxicology
[3]Institute for Diabetes and Regeneration Research
[4]Department of Protein Science
Helmholtz Zentrum München, 85764 Neuherberg, Germany
[5]Welcome Trust Sanger Institute, CB10 1SA Cambridge, UK
[6]Centre for Neuroregeneration Research, School of Molecular and Clinical Medicine, The University of Edinburgh, EH16 4TJ Edinburgh, UK
[7]Centre for Ophthalmology, Institute for Ophthalmic Research, University of Tuebingen, 72076 Tuebingen, Germany
[8]These authors contributed equally to this work
*Correspondence: heiko.lickert@helmholtz-muenchen.de
DOI 10.1016/j.devcel.2011.08.003

## SUMMARY

**The *Drosophila* Discs large (Dlg) scaffolding protein acts as a tumor suppressor regulating basolateral epithelial polarity and proliferation. In mammals, four Dlg homologs have been identified; however, their functions in cell polarity remain poorly understood. Here, we demonstrate that the X-linked mental retardation gene product Dlg3 contributes to apical-basal polarity and epithelial junction formation in mouse organizer tissues, as well as to planar cell polarity in the inner ear. We purified complexes associated with Dlg3 in polarized epithelial cells, including proteins regulating directed trafficking and tight junction formation. Remarkably, of the four Dlg family members, Dlg3 exerts a distinct function by recruiting the ubiquitin ligases Nedd4 and Nedd4-2 through its PPxY motifs. We found that these interactions are required for Dlg3 monoubiquitination, apical membrane recruitment, and tight junction consolidation. Our findings reveal an unexpected evolutionary diversification of the vertebrate Dlg family in basolateral epithelium formation.**

## INTRODUCTION

During embryogenesis, acquisition of cell polarity is essential for epithelium formation, asymmetric cell division, or directed cell migration. Loss of cell polarity is one of the hallmarks of cancer progression. Genetic studies conducted in *Drosophila* led to the identification of three cytoplasmic scaffolding proteins required for both the control of cell polarity and proliferation: Discs large (Dlg), Lethal giant larvae (Lgl), and Scribbled (Scrib). In larvae that have a single mutation in one of these neoplastic tumor suppressor genes, epithelial cells from the imaginal discs and the brain lobes overgrow, whereas loss of cell polarity leads to metastatic tumor formation (Bilder et al., 2000). Dlg, Scrib, and Lgl are essential to establish basolateral polarity and function at the septate junction (SJ; Woods et al., 1996). In contrast, apical polarity is established by the Crumbs complex (Roh et al., 2003; Tepass et al., 1990) in conjunction with the PAR-aPKC (*par*titioning defective-*a*typical *p*rotein *k*inase *C*) complex (Ohno, 2001), which both counteract the activity of the Dlg-Lgl-Scrib complex.

In vertebrate epithelial cells the apical junctional complex (AJC) is formed by the apical tight junction (TJ) and the more basally localized adherens junction (AJ; Shin et al., 2006; Tepass, 2003). The TJ functions as a fence separating the apical from the basolateral membrane domain and also constitutes a barrier against fluid diffusion. The AJ Cadherin-Catenin complex ensures cell-cell adhesion (Aberle et al., 1996). Both apical polarity complexes, Crumbs and PAR-aPKC, play crucial roles in the formation of the AJC and the maintenance of tissue architecture (Lemmers et al., 2004; Suzuki et al., 2001). The Crumbs complex is located apically (Tanentzapf and Tepass, 2003), whereas the PAR-aPKC complex is localized close to the AJC (Izumi et al., 1998). The Dlg complex is localized on the basolateral membrane below the AJC (Naim et al., 2005). Given that the *Drosophila* Dlg localizes to the SJ (Woods et al., 1996), one might expect the vertebrate Dlgs to localize and function at the functional analog TJ. This apparent discrepancy illustrates the fact that the membrane recruitment and molecular functions of the vertebrate Dlg complexes in apical-basal (AB) polarity and AJC formation are far from being understood.

In mammals, four Dlgs have been identified. These belong to the MAGUK (*m*embrane *a*ssociated *gu*anylate *k*inase) family of adaptor proteins and contain three different types of protein-protein interaction (PPI) domains: three postsynaptic density-95/DLG/zonula occludens-1 (PDZ) domain, one Src homology domain-3 (SH3), and one guanylate kinase-like (GUK) domain. The Dlgs act, via these PPI domains, as scaffolds to organize membrane regions and regulate ion channels, signaling

molecules or other adaptor proteins (Sans et al., 2003). Several knockout (KO) studies in mice highlighted a major role for the Dlg homologs in central nervous system activity (Cuthbert et al., 2007; Migaud et al., 1998), and accordingly, loss-of-function mutations in human *DLG3* causes nonsyndromic X-linked mental retardation (Tarpey et al., 2004). Several studies demonstrated an important role for Dlg1 during embryonic and organ development (Caruana and Bernstein, 2001; Mahoney et al., 2006). Nevertheless, it remains unclear whether all mammalian Dlgs function in establishing basolateral epithelial polarity or whether they have functionally diverged during evolution.

The Nedd4 (*n*eural precursor cell-*e*xpressed *d*evelopmentally *d*ownregulated 4) family of ubiquitin ligases (E3) consists of nine members in mammals. The ancestral ligases Nedd4 and Nedd4-2 are most closely related to each other and consist of a N-terminal calcium/lipid and/or protein-binding C2 domain, three to four WW (Tryptophan Tryptophan; Bork and Sudol, 1994) PPI domains, and a C-terminal HECT (*H*omologous to *E*6-AP *C* *T*erminus of the human papilloma virus) ubiquitin-ligase domain (Huibregtse et al., 1995). Both Nedd4 and Nedd4-2 have identical specificity for ubiquitin-conjugating enzymes (Fotia et al., 2006) and bind PPxY (PY) motifs in their key substrates via their WW domains (Kanelis et al., 2001, 2006; Staub et al., 1996). In mammals many potential substrates and/or binding partners of the Nedd4 family have been described, including neurotransmitter channels, growth factor receptors, and signaling proteins. Adaptor proteins contribute to the specificity, diversity, and overall function of both Nedd4 and Nedd4-2; thus, identification and biochemical characterization of interactors greatly facilitate our understanding of these E3 ligases.

Here, we describe that Dlg3 contributes to the establishment of AB and planar cell polarity (PCP) in the mouse embryo. We further identify Nedd4 and Nedd4-2 as Dlg3 interactors and establish that this interaction results in Dlg3 monoubiquitination and apical membrane recruitment. Importantly, we demonstrate that the Dlg3-Nedd4(-2) PPI promotes TJ formation and has contributed to paralog diversification among Dlgs.

## RESULTS

### Homozygous Dlg3 Mutations Cause Midgestational Embryonic Lethality

We recently identified *Dlg3* in a screen for X-linked genes required for mouse embryonic development (Cox et al., 2010). A hemizygous male (XY) mouse embryonic stem cell (mESC) line with a gene-trap (GT) insertion in intron 10 of *Dlg3* (*GtP038A02*) was used to generate completely mESC-derived embryos via the tetraploid complementation method (Nagy et al., 1993). At embryonic day (E) 9.0, $Dlg3^{GtP038A02/Y}$ embryos displayed an array of phenotypic severity that ranged from morphologically normal (data not shown) to a failure of embryonic turning (n = 5 out of 18, Figure 1C), which was associated in rare cases with lack of anterior neural induction (n = 1 out of 18; Figure 1D).

To confirm our findings, we intercrossed hemizygous male and heterozygous female mice carrying a null $Dlg3^{tm1Grnt}$ allele on the inbred C57BL/6 background (Cuthbert et al., 2007). The examination of *Dlg3* mutant embryos at various stages of development revealed no discernible defects prior to E8.0 (see Figure S1A available online). From E8.5 onward, *Dlg3* mutants are statistically underrepresented, and recovered mutants displayed incompletely penetrant defects in embryonic turning, failure of chorioallantoic fusion, posterior truncations (n = 16 out of 38), and lack of anterior neural induction (n = 6 out of 38; Figures 1A and 1B). $Dlg3^{tm1Grnt}$ null embryos also show occasionally an open brain phenotype (n = 8 out of 38; Figures S1B and S1C). Taken together, both the $Dlg3^{GtP038A02}$ and $Dlg3^{tm1Grnt}$ mutant alleles cause embryonic lethality with low penetrance.

### Dlg3 Contributes to AB Polarity in the Mesendodermal Lineage and PCP in the Inner Ear

In a mESC <-> tetraploid embryo chimera wild-type (WT) tetraploid cells contribute only to extraembryonic tissues, such as yolk sac and placenta, and to the gut tube of the early embryo (Figure 1E; Kwon et al., 2008; Tam and Rossant, 2003). Surprisingly, when tetraploid complementation experiments were performed using the $Dlg3^{GtP038A02/Y}$ mutant mESC line (n = 29 chimeras generated in three independent experiments), WT tetraploid cells contributed more extensively to the epithelial lineages of the endoderm, including the fore- (n = 17), mid- (n = 22), and hindgut (n = 28; Figures 1F and 1H–1K), when compared to control experiments (Figures 1E and S1F). In a subset of chimeras, WT tetraploid cells were also found in axial mesendoderm tissues, namely the prechordal plate, notochord, and ventral node (n = 11; Figures 1F, 1G, 1K, and S1F). This contribution is specific because it was never observed in chimeras produced with 68 other X-linked GT mutant mESC lines (Cox et al., 2010) and rescues the Dlg3 mutant phenotype. Our chimera analysis suggests that Dlg3 acts cell autonomously in the axial mesendoderm and definitive endoderm lineages: organizer tissues required for neural induction, neural tube patterning and closure, as well as embryonic turning.

Lack of Dlg3 may result in defects in definitive endoderm and axial mesendoderm specification and/or morphogenesis. To discriminate between these possibilities, we examined differentiation of these tissues using the Forkhead transcription factor Foxa2 (Ang and Rossant, 1994) as a marker. Embryos were also stained with an antibody directed against the apical cilia marker, Arl13b (Caspary et al., 2007), to distinguish the axial mesendoderm (notochord) from the definitive endoderm. Before E8.0, the axial mesendoderm and definitive endoderm lineages were established at comparable ratios, and no obvious morphological defects were discernible between WT and *Dlg3* mutant embryos (data not shown). At E8.5, we frequently observed an enlarged ventral node region and kinked axial midline in mutant embryos (8 out of 14; Figures 1L–1O), suggesting that the axial mesendodermal elongation movement had failed.

To understand the origin of the node cell accumulation, we examined the localization of AB polarity and AJC markers in the mutant embryos. In WT posterior notochord cells, the AJ protein E-cadherin is localized along the basolateral regions of the PM (Figures 2A–2C) but is mislocalized at the apical PM in mutant cells (Figures 2D–2F and S2G–S2I). Similar results were observed with the TJ marker ZO-1 (Figures 2G–2L and S2I) and apical polarity marker aPKC (Figures 2M–2R and S2I). Loss of Dlg3 slightly, but significantly, increases the overall cell proliferation, whereas the apoptosis rate is unchanged (Figures S2A–S2F). Because no changes in proliferation rate were

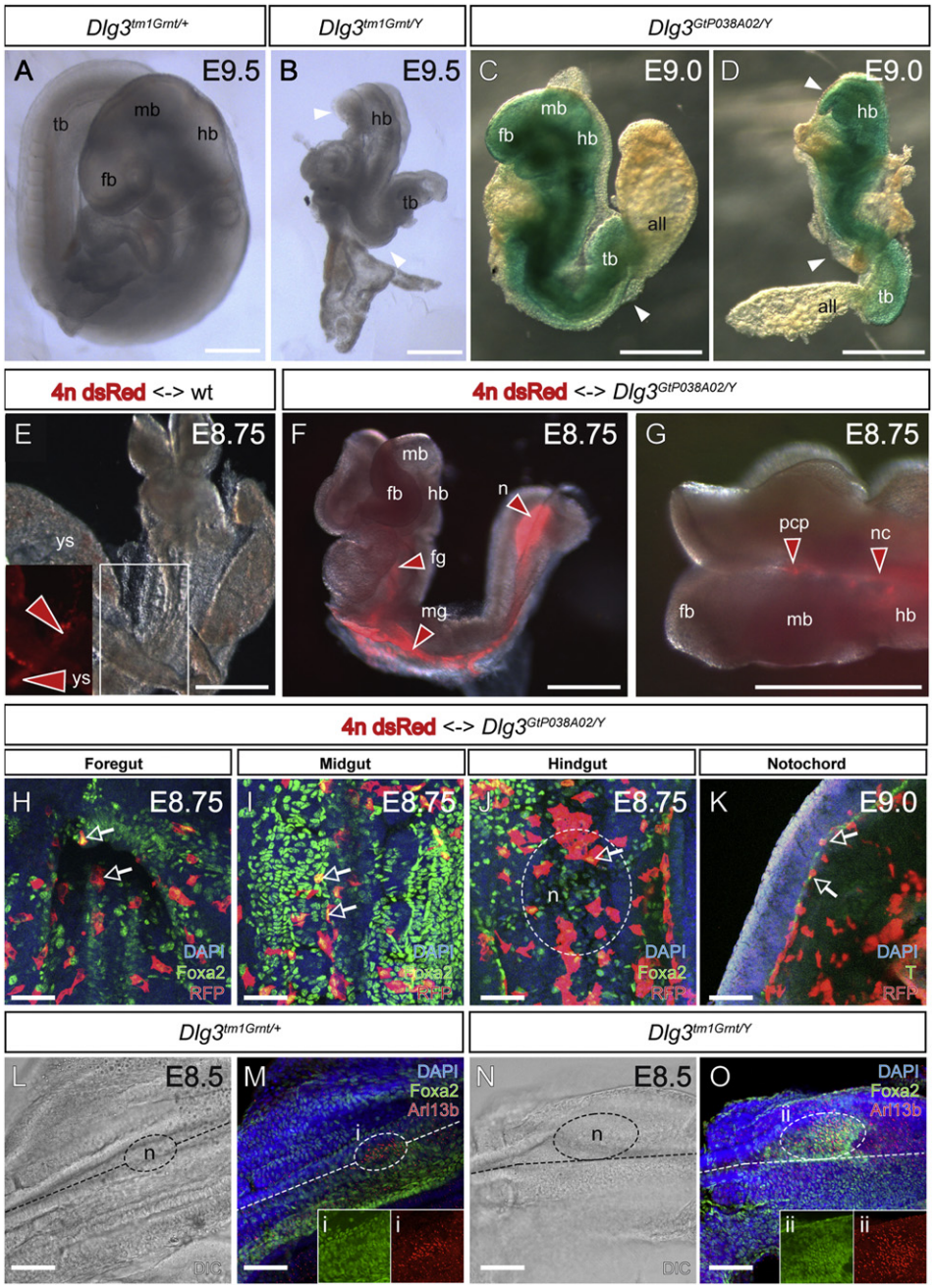


**Figure 1. Homozygous *Dlg3* Mutations Cause Midgestational Embryonic Lethality**

(A–D) Lateral views of (A) WT and (B–D) *Dlg3* homozygous mutant embryos at E9.0–E9.5. Note the similarity of the phenotype observed with the two different *Dlg3* mutant alleles: (B) $Dlg3^{tm1Grnt}$ and (C and D) $Dlg3^{GtP038A02}$. White arrowheads indicate the tail bud (tb) truncation, absence of embryo turning, unfused allantois (all), and in some embryos forebrain (fb) and midbrain (mb) deletions, whereas the hindbrain (hb) remains intact. At E9.0, the GT *β-galactosidase* (*lacZ*) reporter gene is expressed ubiquitously.

(E–K) WT tetraploid embryos expressing a DsRed transgene were aggregated with (E) WT or (F–K) $Dlg3^{GtP038A02/Y}$ mESCs and isolated at E8.75–E9.0. (E–G) Red arrowheads indicate WT tetraploid cells (red) contributing to (E) the yolk sac (ys) or to (F and G) the node (n), midgut (mg), foregut (fg), notochord (nc), and prechordal plate (pcp). (H–K) Chimeras were immunostained with anti-RFP (red) in combination with anti-Foxa2 or anti-T (green) antibodies. DAPI (blue) has been used to mark all nuclei. Optical sections were taken at the level (H) of the foregut, (I) midgut, (J) hindgut (node outlined by broken oval), and (K) notochord. White arrows indicate tetraploid WT cells, expressing (H–J) the endoderm marker Foxa2 or (K) the notochord marker T.

(L–O) Whole-mount immunofluorescence combined with confocal imaging. Ventral views of the hindgut and node region in (L and M) WT and (N and O) *Dlg3* homozygous mutant embryos at E8.5. White dashed lines and ovals mark the midline and the node, respectively. Embryos were stained with DAPI (blue) and with Foxa2 (green) and Arl13b (red) antibodies. At the level of the node, some *Dlg3* mutants present a lateral expansion of Foxa2 and Arl13b-positive cells compared to the WT (compare i and ii). Scale bars represent 300 μm in (A)–(G), 50 μm in (H)–(K), and 75 μm in (L)–(O).

See also Figures S1 and S2.

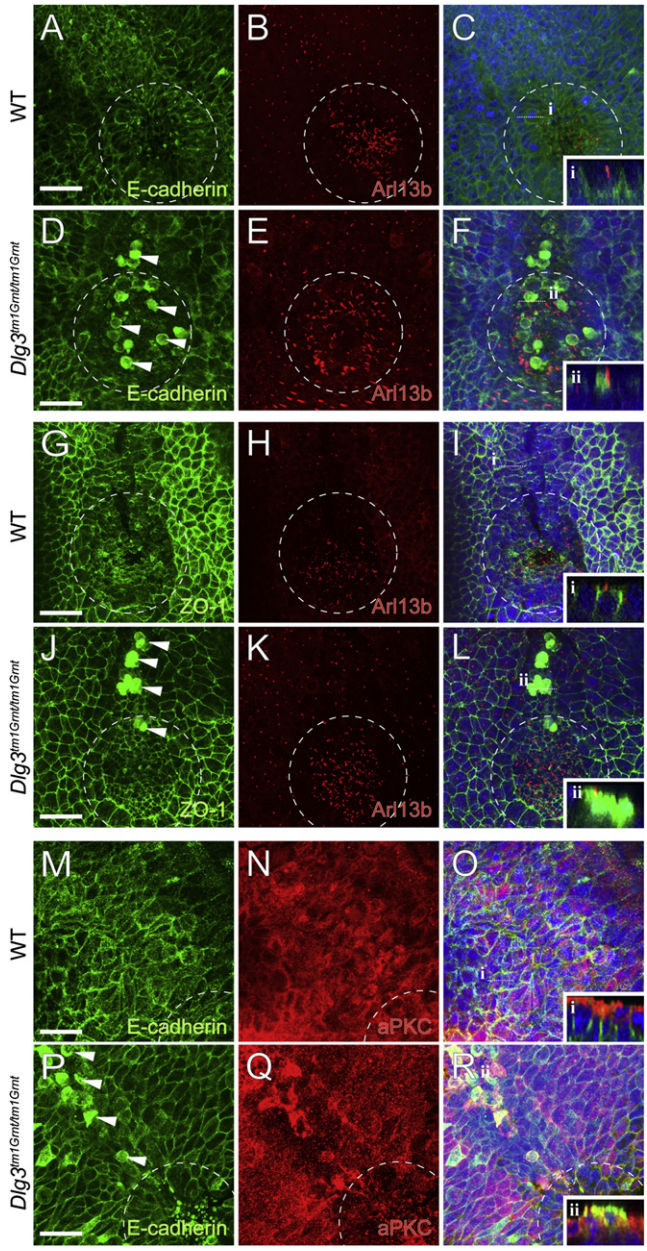


**Figure 2. Loss of AB Cell Polarity in *Dlg3* Mutant**

WT and *Dlg3* mutant embryos were whole-mount immunostained with the indicated antibodies, and nuclei were marked with DAPI (blue) at E8.5. White dashed ovals indicate the node. The levels of transverse optical sections (i and ii) are marked by white dashed lines. Pictures show ventral views on the mouse node with the anterior facing up.

(A–F) Expression of the cilia marker Arl13b (red) and the AJ marker E-cadherin (green) in WT and *Dlg3* mutant embryos. Note the loss of basolateral localization of the AJ marker E-cadherin in *Dlg3* mutant cells indicated by arrowheads (i and ii).

(G–L) Overlapping expression of cilia (Arl13b; red) and TJ (ZO-1; green) markers in *Dlg3* mutant embryos in comparison with WT. Loss of cell polarity is visible in higher magnification images (compare i and ii).

(M–R) Expression of apical epithelium (aPKC; red) and AJ (E-cadherin; green) in WT and *Dlg3* mutant embryos. Note the ectopic localization of E-cadherin in the apical PM (compare i and ii). Cells losing AB polarity are positive for the axial mesendoderm and definitive endoderm marker Foxa2 (data not shown; Figures S2G and S2H).

observed in the axial mesendoderm (data not shown), enlargement of the node region in *Dlg3* mutants could result from abnormal anterior-posterior (AP) elongation of the notochord, which depends on PCP-mediated convergence and extension movements. To seek evidence for a possible function of Dlg3 in PCP, we investigated tissue polarity in the inner ear, which revealed clear defects in Dlg3 mutant embryos at E18.5 (Figures S1D and S1E). Thus, analogous to *Drosophila* Dlg, mammalian Dlg3 influences both AB polarity (Woods et al., 1996) and PCP (Bellaïche et al., 2001).

## The Mammalian Dlg1–Dlg4 Show Different Tissue-Specific and Subcellular Localization

Within the Dlg family, Dlg3 shows the earliest reported polarity phenotype. To dissect possible functional differences and redundancies between individual Dlgs, we investigated the mRNA expression of *Dlg1–Dlg4* during early mouse development. Reverse transcriptase-polymerase chain reaction (RT-PCR) analysis revealed that all four *Dlgs* are expressed from gastrulation to the onset of organogenesis (Figure 3A). Whole-mount in situ hybridizations showed that at E8.5, *Dlg1*, *Dlg3*, and *Dlg4* are expressed in the tail bud region at the junction where presomitic mesodermal cells undergo mesenchymal-epithelial transition to condense and form segmented somites (Figure 3B). All *Dlgs* are expressed in epithelial neuroectodermal cells of the head region, whereas *Dlg2*, *Dlg3*, and *Dlg4* are also expressed in the epithelial lining of the gut along the AP axis (Figure 3B). Thus, the tissue-specific expression of the different *Dlg* family members suggests a partially redundant function in epithelial polarization in all three germ layers.

Next, we characterized the tissue distribution and the subcellular localization of the Dlg proteins during gastrulation at E7.5. Dlg1 is localized to all three germ layers, whereas Dlg2, Dlg3, and Dlg4 show higher abundance in the mesoderm and endoderm compartment (Figure S3). The four Dlgs are found at cell junctions in epithelial cell types, but interestingly, these proteins are also present at clearly distinct intracellular localizations (Figures 3C–3F). In ventral node cells only Dlg1 expression is restricted to the basolateral membrane of epithelial cells, analogous to *Drosophila* Dlg (Figure 3C). In contrast, Dlg2 and Dlg3 are located along the cell membrane with a peak in distribution at the level of the apical membrane (Figures 3D and 3E). Dlg4 is found along the PM and is not restricted to a particular compartment (Figure 3F).

In stable transfected and polarized Madine Darby canine kidney (MDCK) cells, a N-terminal tagged Strep-Flag-Dlg3 (SF-Dlg3) localizes to both cytoplasm and membrane, comparable to endogenous Dlg3 in mouse embryos (compare Figures 3E and 3G). Whereas Dlg1 is strictly localized to the basolateral membrane (Figure 3H), Dlg3 membrane localization extends to the apical apex and AJC, where it colocalizes with TJ markers (Figures 3I ad 3J). These unexpected findings suggest that during evolution the different Dlgs have acquired paralog-specific functions in the consolidation of polarized membrane domains.

Scale bars represent 25μm.
See also Figures S1 and S2.

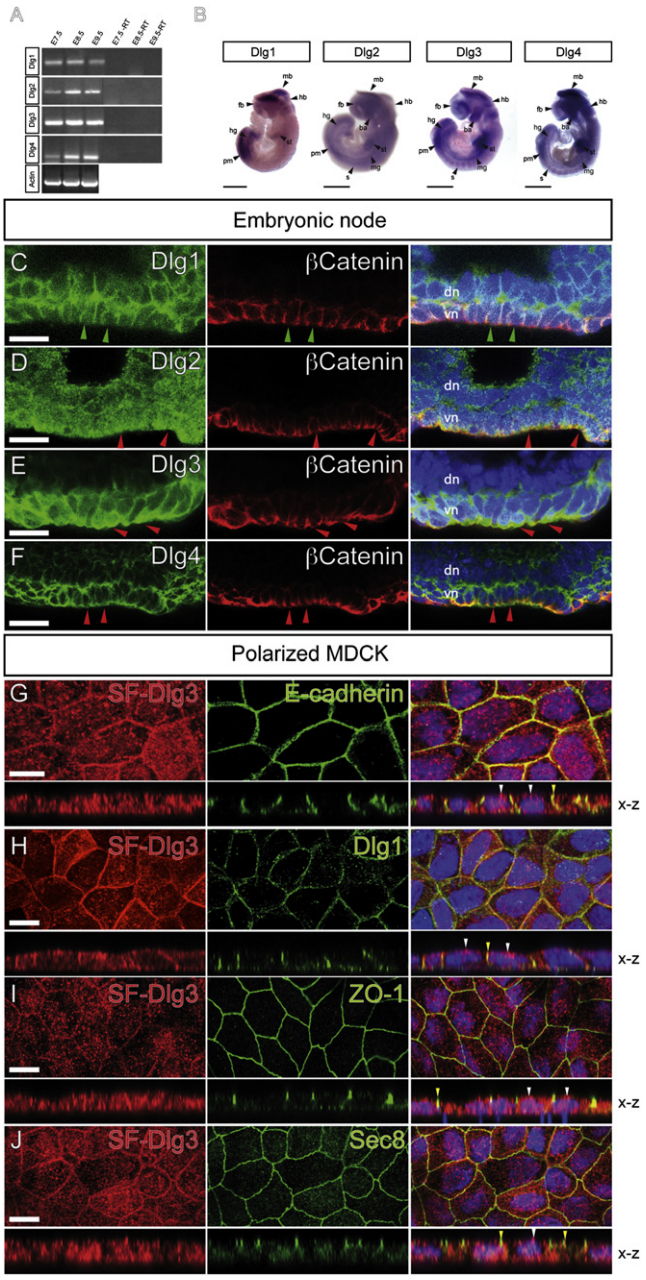


**Figure 3. The Mammalian Dlg1–Dlg4 Show Distinct mRNA Expression and Protein Localization**

(A) RT-PCR analysis of the *Dlg* mRNA expression at E7.5–E9.5. Expression of *Actin* mRNA has been used for normalization.

(B) Whole-mount in situ hybridization analysis of the four *Dlgs*' mRNA at E8.5. Note that the *Dlgs* are expressed in regions of epithelial-mesenchymal and mesenchymal-epithelial transition. fb, forebrain; mb, midbrain; hb, hindbrain; ba, branchial arches; st, septum transversum; mg, midgut; s, somites; pm, presomitic mesoderm; hg, hindgut.

(C–F) Whole-mount localization studies of the Dlg proteins and the AJ marker β-catenin in ventral (vn) and dorsal (dn) node cells. (C) Dlg1 colocalizes with β-catenin at the basolateral PM and cell junctions. Note the absence of Dlg1 at the apical PM (green arrowheads). (D and E) Dlg2 and Dlg3 are expressed in the cytoplasm and along the PM with a higher expression at the apical region (red arrowheads). (F) Dlg4 is present all around the PM, including the apical domain (red arrowheads).

(G–J) Immunolocalization studies of stably expressed SF-Dlg3 in polarized MDCK cells. Cells were stained against Flag-epitope (red) in combination with antibodies specific for polarity markers (green). Note that, contrary to Dlg1, SF-Dlg3 is not restricted to the basolateral membrane and is also found at the TJ marked by ZO-1 and Sec8 (yellow arrowheads) and at the apical membrane (white arrowheads).

Scale bars represent 500 μm in (B), 25 μm in (C)–(F), and 10 μm in (G–J).

See also Figure S3.

## Identification of the Dlg3 Interactome in Polarized Epithelial Cells

With the goal of understanding Dlg paralog diversification, we screened for Dlg3 interaction partners in polarized MDCK cells that establish fully functional junctions when grown at high density. We performed tandem affinity purification (TAP) using SF-Dlg3 in conditions optimized for the native purification of protein complexes (Gloeckner et al., 2007). As a control, TAPs were performed in parallel with untransfected MDCK cells. The purified proteins were identified by liquid chromatography coupled with tandem mass spectrometry (LC-MS/MS).

The identified Dlg3 interactome consists of polarity-associated proteins such as the TJ-associated protein 1 (TJAP1/Pilt), a known interaction partner of Dlg1 (Kawabe et al., 2001) and Dlg2, which shows similar apical localization as Dlg3 (Figure 4A). Furthermore, we identified the protein phosphatase 1 that has been recently described as being part of an AJC regulating Par-3/aPKC activity (Hendrickx et al., 2009; Traweger et al., 2008) and the motor protein Dynein required for vectorial transport of vesicles to the apical surface (Lafont et al., 1994). We also identified potential interactions of Dlg3 with Nedd4-2, an E3-ubiquitin ligase involved in protein trafficking, and the Nedd4-binding protein 3 (N4BP3; Murillas et al., 2002), a scaffolding protein that recruits Nedd4. These observations, in combination with our in vivo findings, strongly suggest a function of Dlg3 and possibly also Nedd4(-2) in cell polarity and AJC formation.

## Dlg3 Interaction with the E3-Ubiquitin Ligases Nedd4 and Nedd4-2 Increases during Cell Polarization

To characterize the Dlg3-Nedd4(-2) interaction, we immunoprecipitated recombinant SF-Dlg3 from polarized MDCK cells. Using antibodies specific to the Nedd4 ubiquitin ligases (Nedd4 and Nedd4-2) on immunoblots of the Strep eluate, we detected endogenous Nedd4 and Nedd4-2, confirming our TAP findings (Figure 4B). The interaction of Dlg3 with the Nedd4 protein was confirmed in vivo by coimmunoprecipitation (coIP) of the endogenous Nedd4 ligases from brain tissues together with Dlg3 (Figure 4C). During epithelial polarization subconfluent cells first establish E-cadherin mediated contacts that correspond to the ensuing AJs. This is followed by recruitment of TJ-associated proteins. Evidence from our interactome studies suggests that Dlg3 and Nedd4(-2) E3 ligases may establish polarization-dependent protein associations (Figures 4A and 4B). To test this hypothesis, we immunoprecipitated SF-Dlg3 from stable MDCK transfectants grown under unpolarized or polarized conditions. We observed that higher levels of endogenous Nedd4(-2) ligases were pulled down from polarized cells compared to unpolarized cells (Figures 4D and 4E).

Immunolocalization studies in MDCK transfectants revealed that Nedd4(-2) and Dlg3 colocalize in the cytoplasm (Figure 4F

A

| MS/MS identified proteins | Accesion number | Peptides | Nature |
|---|---|---|---|
| Discs large homolog 2 (Dlg2) | XP_542276 | 1 | scaffolding protein |
| Tight junction associated protein 1 (TJAP1) | XP_538937 | 1 | scaffolding protein |
| Nedd4-binding protein 3 (N4BP3) | XP_538567 | 1 | scaffolding protein |
| E3 ubiquitin-protein ligase NEDD4-like (NEDD4l) | XP_850792 | 2 | enzyme |
| Protein phosphatase 1a/2a (PP1a/2a) | NP_001003064 | 2 | enzyme |
| Dynein intermediate chain (Dynein IC) | XP_859859 | 2 | motor protein |

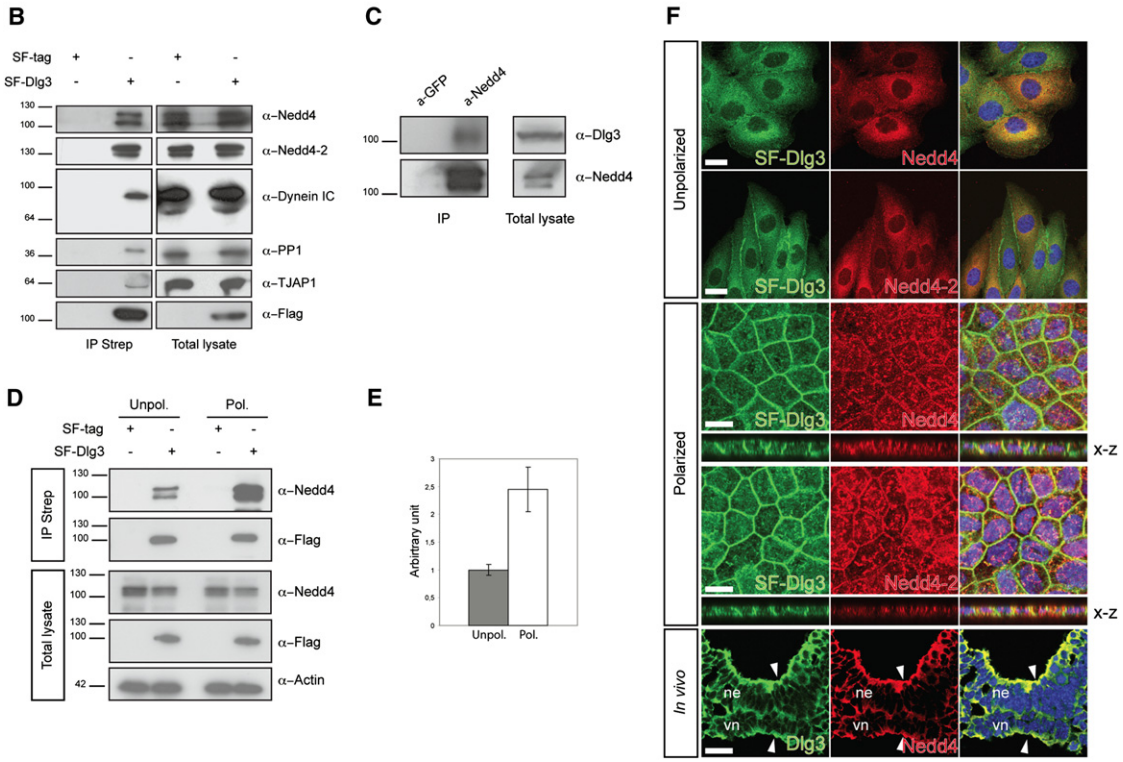


**Figure 4. Dlg3 Interacts with Cell Polarity and TJ-Associated Proteins**

(A) Interactome of Dlg3-binding proteins in polarized MDCK cells.

(B) Confirmation of the identified Dlg3 interactome. The SF-tagged Dlg3 was immunoprecipitated from stably transfected MDCK cells using Streptavidin affinity beads (IP Strep). The total lysate (right panel) and the IP (left panel) were split and subjected to anti-Nedd4, anti-Nedd4-2, anti-PP1, anti-TJAP1, anti-Dynein intermediate chain (IC), and anti-Flag via western blotting. Note the specific detection of endogenous Nedd4 (two isoforms), Nedd4-2 (two isoforms), PP1, TJAP1, and Dynein IC in the IP. MDCK cells expressing the SF tag alone were used as negative control.

(C) The Nedd4 ubiquitin ligases interact with Dlg3 in vivo. Brain tissues were used to specifically immunoprecipitate (IP) endogenous Nedd4. The lysate and IP were split and subjected to anti-Dlg3 (top panel) and anti-Nedd4 (bottom panel). An anti-GFP antibody was used as a specificity control.

(D and E) Dlg3 and Nedd4 interaction increases with polarization. SF-Dlg3 was immunoprecipitated (IP Strep) from unpolarized (Unpol.) or polarized (Pol.) MDCK cells. Equivalent amounts of SF-Dlg3 bait were pulled down from the different samples. Note that the amount of Nedd4 ligases immunoprecipitated is higher in polarized cells in comparison with unpolarized cells. Five percent input of the total lysate is shown as a loading and specificity control. (E) Data from three independent experiments were compiled and quantified using Photoshop. Interaction strength in the unpolarized conditions is arbitrarily set to 1. Errors bars indicate standard deviation in the graphs (mean ± SD; $p < 0.05$).

(F) Colocalization studies of Dlg3 and the Nedd4 ligases during epithelial polarization. In unpolarized MDCK cells, SF-Dlg3 and Nedd4/Nedd4-2 localize mainly in the cytoplasm (top panels; scale bar, 10 μm). In polarized MDCK cells, Dlg3 and Nedd4/Nedd4-2 colocalize at the PM and in the cytoplasm (middle panel; scale bar, 10 μm). Transverse cryosection stained for Dlg3 and Nedd4(-2) at the level of the node at E8.5 (bottom panel; scale bar, 25 μm). Note the colocalization of Dlg3 and Nedd4 at the apical PM (white arrowheads). ne, neurectoderm; vn, ventral node.

See also Figure S4.

and S4A–S4F), whereas polarization led to an increased colocalization at the apical membrane and AJC (Figure 4F). This is consistent with the colocalization of Dlg3 and Nedd4(-2) at the apical PM of neural ectoderm and ventral node cells at E8.5 (Figure 4F). Taken together with the fast recruitment of Dlg3 to the apical PM and TJ in a repolarization assay (Figures S4G–S4L), these data suggest that the Dlg3-Nedd4(-2) interactions might be important for membrane recruitment during cell polarization. Importantly, both the PPI with the apical transport motor protein Dynein IC (Figure 4B) and the Sec8 component of the exocyst complex (Figure 6B) depend on functional Dlg3-Nedd4(-2) interactions (see below).

### Dlg3 Is the Only Dlg Family Member Containing PY Motifs for Nedd4(-2) Ligase Binding

To map the Dlg3 interaction domain with the Nedd4(-2) ligases, we used a series of different Dlg3 deletion mutants in coIP experiments (Figure 5A). We observed that the PDZ domain of Dlg3 weakly binds to the endogenous Nedd4(-2) ligases, whereas Dlg3ΔPDZ does not. In contrast the deletion mutants of Dlg3 that were missing either the SH3 or GUK domain remained capable of binding the endogenous Nedd4 and Nedd4-2 (Figure 5A).

A large number of Nedd4 interactors contain PY motifs that mediate direct interaction with the WW domains of Nedd4 proteins (Kanelis et al., 2001, 2006). Sequence analysis of Dlg proteins revealed that Dlg3 contains two PY motifs, which are located before and in between the Nedd4(-2) interacting PDZ domains (Figure 5C). Point mutations that resulted in an amino acid substitution of Tyrosine for Alanine in both PY motifs completely abolished the interaction of Dlg3 with endogenous Nedd4(-2) proteins (Figure 5B). Another remarkable feature was the conservation of the Dlg3 PY motifs in vertebrates (Figure 5C), even though these motifs are absent in other mammalian Dlgs and in *Drosophila* Dlg (Figure S5). We observed that only Dlg3 is capable of binding to the Nedd4 and Nedd4-2 proteins (Figure 5D).

### Nedd4 Directly Catalyzes Dlg3 Monoubiquitination

Given the known function of the E3-ubiquitin ligase Nedd4 in protein trafficking by monoubiquitination and in targeted protein degradation by polyubiquitination, we tested the capacity of NEDD4 to mediate Dlg3 ubiquitination. In the presence of NEDD4 and after SF-Dlg3 IP after very stringent SDS boiling conditions, we observed a slightly retarded band that is detected with an anti-Flag as well as an anti-ubiquitin antibody, providing evidence that NEDD4 can catalyze Dlg3 monoubiquitination (Figure 6A). A catalytically inactive form of NEDD4, NEDD4(C-A)-Myc, which still associates with Dlg3, cannot promote SF-Dlg3 monoubiquitination (Figures 6A and S6).

We used a series of Dlg3 mutants to map the region targeted for monoubiquitination by NEDD4 (Figure S6A). The Dlg3 mutant for the NEDD4-binding motif (SF-Dlg3$^{YA1+2}$) cannot be monoubiquitinated, providing further evidence that Nedd4 directly targets Dlg3. The SF-PDZ alone is not modified by ubiquitin, which could either be due to an inefficient association with Nedd4 (Figure 5A), or it may indicate that ubiquitination takes place outside of this region. Thus, we determined ubiquitination in C-terminal Dlg3 deletion mutants that are efficiently interacting with Nedd4 (Figure 5A). Whereas deletion of the GUK did not affect the extent of monoubiquitination, removal of the SH3 domain caused a complete loss of NEDD4-mediated ubiquitin attachment (Figure S6A). These results suggest that lysines within the SH3 domain are either directly targeted for ubiquitin modification by NEDD4, or the removal of the SH3 domain exerts a conformational change that prevents ubiquitin attachment to Dlg3.

### Dlg3-Nedd4(-2) Association Regulates Intracellular Trafficking via the Exocyst Complex to Contribute to Polarity and TJ Consolidation

During epithelialization the targeting of membrane-associated proteins to cell junctions is controlled by the exocyst pathway (Hsu et al., 1999). Dlg3 interacts with the exocyst component Sec8 to regulate microtubule (MT)-dependent neurotransmitter intracellular trafficking from the endoplasmic reticulum to the synaptic membrane (Sans et al., 2003). We found that the interaction of Dlg3 with the exocyst and Dynein apical transport motor protein complexes also occurs in polarized MDCK cells and specifically depends on the capacity of SF-Dlg3 to bind the Nedd4(-2) ligases, whereas interaction with PP1 was not affected by the PY mutations (Figure 6B).

To test whether Dlg3-Nedd4(-2) binding is involved in targeted delivery of proteins to the apical membrane and TJ, we derived cysts from untransfected MDCK cells and from MDCK cells that stably expressed SF-Dlg3 or SF-Dlg3$^{YA1+2}$. We observed that SF-Dlg3$^{YA1+2}$ overexpression results in abnormal polarization of the MDCK cysts, whereas SF-Dlg3 overexpression does not (Figure S6C). In contrast to SF-Dlg3, SF-Dlg3$^{YA1+2}$ mislocalizes to the basolateral PM of MDCK cells and is absent from both the apical membrane and TJ (Figure S6C). Using a combination of different siRNAs designed to knock down Nedd4 and/or Nedd4-2 (Figures 6C and 6E–6G), we could confirm that Nedd4 and Nedd4-2 are required for TJ formation in polarized MDCK cells (Figures 6D, 6H, and 6I).

Finally, we tested the functional impact of the Dlg3-Nedd4(-2) interaction in vivo. We stably expressed equal levels of SF-Dlg3 and SF-Dlg3$^{YA1+2}$ in embryonic stem cells (ESCs) (Figure 7A) and performed tetraploid complementation to generate completely ESC-derived embryos. Strikingly, the overexpression of the SF-Dlg3$^{YA1+2}$ Nedd4(-2)-binding mutants dominantly interfered with convergent and extension-mediated axis elongation, whereas the overexpression of SF-Dlg3 had no discernible effect on embryonic development between E7.75 and E8.5 (Figure 7B). On the cellular level the SF-Dlg3$^{YA1+2}$ Nedd4(-2)-binding mutant did not reach the apical PM and TJ (Figures 7C–7F), thereby affecting mainly TJ formation in the endoderm (Figures 7E and 7F) and mesendoderm (Figure 7G), eventually causing membrane rupturing. Comparable to the *Dlg3* null mutation, the phenotype is specific and restricted to the mesendoderm and endoderm because TJ formation is not affected in other lineages such as the ectoderm (Figure 7H). Altogether, these results strongly suggest that the E3 ligases Nedd4 and/or Nedd4-2 are necessary for the targeted delivery of Dlg3 to the apical membrane to promote cell polarity and TJ consolidation.

## DISCUSSION

We have uncovered a role for functional Dlg3-Nedd4(-2) PPIs in apical epithelial polarity and TJ formation that is supported by several lines of evidence. First, in polarized MDCK cells and in the mouse embryos, Dlg3 and Nedd4(-2) accumulate at the apical membrane domain and TJ. Second, Dlg3 interacts with proteins associated with the formation of apical membrane (PP1, Nedd4, and Nedd4-2) and TJ (TJAP1, Sec8) in polarized MDCK cells and in vivo. Third, the combined knockdown of Nedd4 and Nedd4-2 causes TJ formation defects in polarized MDCK cells; and finally, the mislocalization of the Nedd4(-2)-binding mutant form of Dlg3 causes severe polarization and TJ formation defects in MDCK cells and mouse embryos.

These observations contrast with the current view that the Dlgs function exclusively at the basolateral membrane, which

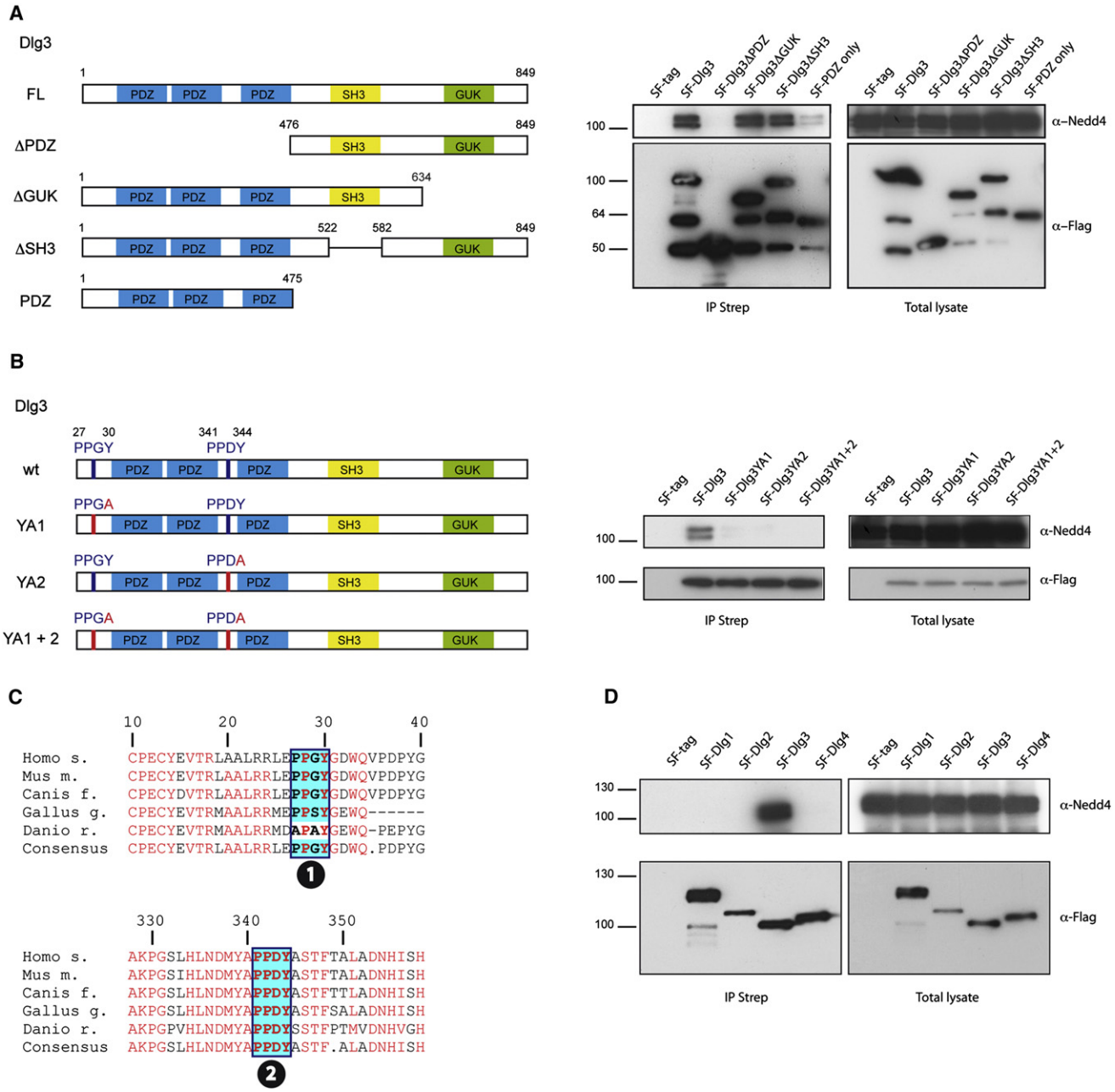


**Figure 5. Dlg3, but Not Dlg1, Dlg2, or Dlg4, Interacts with Nedd4 and Nedd4-2**

(A) The PDZ domains of Dlg3 contribute to Nedd4 binding. Different deletion mutants of SF-Dlg3 (left panel) were immunoprecipitated from transiently transfected HEK293T cells via an IP Strep. The total lysate and the IP were split and subjected to anti-Nedd4 and anti-Flag via western blotting. Endogenous Nedd4 was detected in the IP Strep in the presence of full-length SF-Dlg3, SF-Dlg3ΔGUK, SF-Dlg3ΔSH3, and also weakly in the presence of SF-PDZ only. HEK293T cells expressing only the SF tag were used as a negative control. Lower bands correspond to degradation products.

(B) The Nedd4 ligases bind to Dlg3 in a PY motif-dependent manner. Indicated point mutants of Dlg3 PY motifs were generated by exchanging Tyrosine to Alanine and tagged with the SF-tag (left panel). Lysates from HEK293T cells transfected with these expression vectors were subjected to IP Strep. The lysates and IP were analyzed by western blotting using anti-Nedd4 and anti-Flag antibodies. Point mutation of both PY motifs totally abolishes interaction with the Nedd4 ligases.

(C) Multiple species ClustalW alignment of Dlg3 reveals evolutionary conservation of PY motifs (boxed regions) in vertebrates.

(D) Dlg3, but not Dlg1, Dlg2, or Dlg4, interact with the ubiquitin ligases Nedd4 and Nedd4-2. Lysates from HEK293T cells transfected with the mentioned expression vectors were subjected to IP Strep. The lysates and IP were analyzed by western blotting using anti-Nedd4 and anti-Flag antibodies. The same results were obtained using a Nedd4-2 antibody (data not shown).

See also Figure S5.

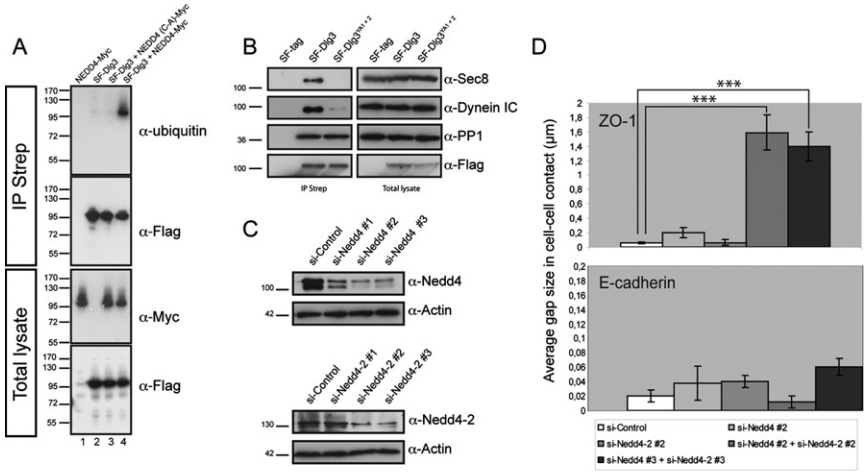


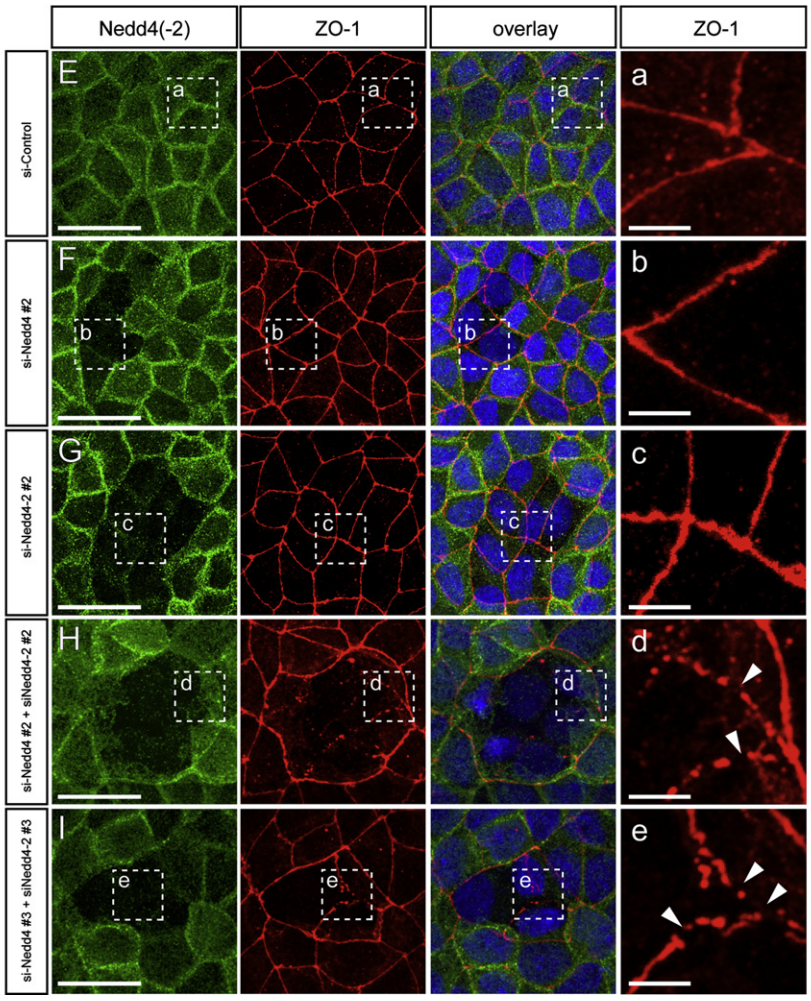


**Figure 6. Nedd4 Directly Targets Dlg3 Monoubiquitination and Regulates Its Function**

(A) In vitro monoubiquitination of Dlg3. HEK293T cells were transfected with the indicated constructs. Cells were lysed in 0.8% SDS containing buffer and boiled for 5 min. Samples were then diluted to 0.1% SDS prior to Strep IP. Precipitates (IP Strep) were analyzed for ubiquitination by western blotting. Expression of the different constructs (total lysate) was controlled by western blotting. Note that in the presence of Nedd4-Myc (lane 4), SF-Dlg3 is monoubiquitinated, whereas the catalytically inactive Nedd4 (C-A)-Myc (lane 3), does not modify SF-Dlg3.

(B) Dlg3 interaction with the exocyst and Dynein depends on Nedd4 binding. Indicated polarized MDCK stable transfectants were lysed and processed for an IP Strep. The total lysate (left panel) and the IP (right panel) were split and subjected to anti-Sec8, anti-Dynein IC, and anti-Flag via western blotting. Endogenous Dynein IC and Sec8 are precipitated in the presence of SF-Dlg3, but not SF-Dlg3$^{YA1+2}$. The Dlg3-PP1 interaction remains unchanged upon PY motif mutations.

(C) Three different siRNA duplexes were designed to knock down Nedd4 (si-Nedd4#1, #2, and #3) or Nedd4-2 (si-Nedd4-2#1, #2, and #3) in MDCK cells. Note that Nedd4 siRNA duplexes #2 and #3 and Nedd4-2 siRNA duplexes #2 and #3 efficiently knock down Nedd4 and Nedd4-2 protein, respectively.

(D) Quantification of average gap size in cell-cell junctions in cells transfected with indicated siRNAs and stained with TJ (ZO-1) and AJ (E-cadherin) markers. Mean ± SD; ***$p < 0.01$.

(E–I) Polarized MDCK cells were transiently transfected with an si-Control (E), si-Nedd4#2 (F), si-Nedd4-2#2 (G), or a combination of siRNAs targeting Nedd4 and Nedd4-2 (H and I). Cells were immunostained with anti-Nedd4 (E, F, H, and I) or anti-Nedd4-2 (G) and anti-ZO-1 antibodies (E–I) and analyzed by confocal microscopy. Boxed areas are shown in high resolution (a–e). (H and I) Note that the combined Nedd4 and Nedd4-2 knockdown specifically affects TJ formation (white arrowheads). Scale bars represent 25 μm in (E)–(I) and 5 μm in higher magnification images (a–e).

See also Figure S6.

is based predominantly on *Drosophila* studies. Despite highly similar protein sequences, the vertebrate Dlgs present heterogeneous expression patterns at both the tissular and subcellular levels of the adult brain (Aoki et al., 2001) and mouse embryo. Because we discovered that Dlg3 is the only Dlg bearing PY Nedd4-binding motifs, the appearance of paralog-specific PPIs is likely to correlate with functional diversification during the molecular evolution of the Dlgs. It is also interesting to note that although the only Dlg in *Drosophila* localizes and functions at the SJ, the recruitment and function of vertebrate Dlg3 at the analogous TJ have evolved independently.

As shown in the graphical abstract, our model proposes that Dlg3-Nedd4(-2) interactions recruit a subfraction of the cellular Dlg3 pool to the apical membrane and TJ in cooperation with motor proteins and trafficking machineries. During polarization, exocyst components connect vesicles exiting the Golgi to

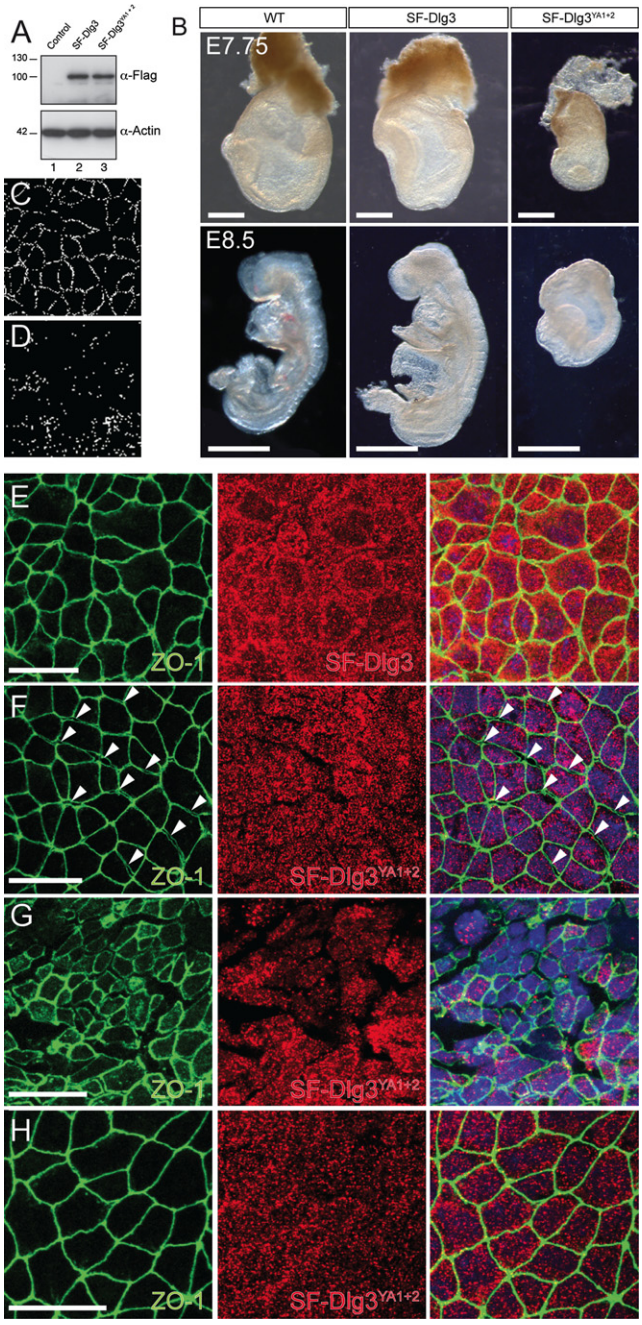


**Figure 7. The Overexpression of the SF-Dlg3$^{YA1+2}$ Nedd4(-2)-Binding Mutants Dominantly Interferes with AB Cell Polarity In Vivo**

(A) Immunoblot (anti-Flag) showing the equal expression of SF-Dlg3 (lane 2) or SF-Dlg3$^{YA1+2}$ (lane 3) proteins in stable ESC clones. Untransfected ESCs are shown as negative control, and Actin served as loading control.

(B) Lateral views of control, SF-Dlg3, and SF-Dlg3$^{YA1+2}$ ESC-derived embryos. Note the axis elongation defects in the SF-Dlg3$^{YA1+2}$ embryos at E7.75 (scale bars, 200 μm) and E8.5 (scale bars, 300 μm).

(C and D) Colocalization of the TJ marker ZO-1 with SF-Dlg3 (C) or SF-Dlg3$^{YA1+2}$ (D) as revealed by quantitative statistical colocalization on two-color confocal images. Raw images used for colocalization measurements are presented in (E) and (F) (overlays).

(E–H) Analysis of TJ formation by whole-mount immunofluorescence in the endoderm (E and F), ventral node (G), and ectoderm (H). Note the epithelial holes (F, white arrowheads) and rupturing (G) in SF-Dlg3$^{YA1+2}$ mutants as compared to the control (E). Scale bars represent 25 μm.

See also the graphical abstract.

membrane-associated proteins and become recruited via MT-dependent transport to forming TJs (Yeaman et al., 2004). We hypothesize that Nedd4(-2)-mediated Dlg3 monoubiquitination takes place in the cytoplasm. Upon Nedd4 interaction, Dlg3 is trafficked via MT together with Sec8, Nedd4(-2), and polarity-associated proteins toward the TJ and apical membrane, consistent with recent findings (Matern et al., 2001; Plant et al., 2000; Sans et al., 2003). The scaffolding protein Dlg3 may then orchestrate the establishment and/or maintenance of discrete membrane domains and TJ through PPIs.

*Dlg3* null embryos exhibit AB polarity defects in the axial mesendoderm, namely the ventral node and notochord, with low penetrance. During gastrulation these cell populations reach the surface of the embryo and acquire an epithelial morphology (Burtscher and Lickert, 2009). Accordingly, KO embryos for another MAGUK, the TJ protein ZO-1, also show axial mesendoderm disorganization (Katsuno et al., 2008). In a subset of *Dlg3* KO embryos, we also observed an accumulation of notochord cells at the level of the node. We hypothesize that due to loss of polarity, these cells are incapable of reaching the anterior region of the embryo. Convergent and extension movement drives AP elongation of the notochord. This not only depends directly on PCP but also indirectly on AB polarity and cell-cell adhesion molecules (Montcouquiol et al., 2003). Our results are consistent with these observations and suggest that Dlg3 contributes to both AB polarity and PCP initiation in the mouse embryo. The Smurf E3 ligases of the Nedd4 family have been recently shown to regulate PCP in the mouse embryo (Narimatsu et al., 2009). In the future it will be interesting to analyze how Nedd4 family members and polarity complexes act together to regulate AB polarity and PCP.

During development the anterior endoderm and axial mesendoderm act together as the late-gastrula organizer essential for anterior induction and head development (Ang and Rossant, 1994; Kinder et al., 2001). Chimera experiments suggest that Dlg3 plays a specific cell-autonomous function in the development of these organizer cell populations. Subsequently, we concluded that the patterning defects observed in Dlg3 KO, namely lack of anterior neural induction, as well as embryonic turning defects and posterior truncation, correspond to secondary defects. We propose that in tetraploid WT embryo <-> mESC *Dlg3* mutant chimeras, anterior visceral endodermal cells from the WT tetraploid host embryo can provide a functional substitute for the defective organizer cell populations. These cell types express inhibitors of the Nodal/TGFβ- and Wnt/β-catenin pathways, which are essential for anteriorization of the neural ectoderm (Egea et al., 2008), and it was recently demonstrated that visceral endoderm cells contribute to the embryo during unperturbed development (Kwon et al., 2008). The extent to which these cells contribute to the embryo correlates with the rescue of the mutant phenotype, suggesting that this is part of the compensatory mechanisms by which some Dlg3 mutants can overcome embryonic lethality. Further explanations for the low-penetrant phenotypes are differences in genetic

background and functional redundancies within and among cell polarity complexes. Because cell polarity is crucially important for development and morphogenesis, nature has compensated for the loss of polarity molecules by gene duplication and diversification. This contributes to functional redundancy among the Dlgs and other families of polarity regulators (Hashimoto et al., 2010; Narimatsu et al., 2009; Klezovitch et al., 2004) but also protects against lethal mutations. An additional advantage of gene duplication is the possibility of diversification. Dlg3 is one example of how evolution creates molecular and functional diversity, i.e., by establishing paralog-specific PPIs.

In human, mutations of *Dlg3* are associated with nonsyndromic X-linked mental retardation (Tarpey et al., 2004). Our findings on the specific role of Dlg3 provide original insights into the etiology of this mental disorder. Defects in the organizer axial mesendoderm tissue in the Dlg3 null embryos result in anterior region malformation with low penetrance. In the less severely affected embryos, abnormal cortical development may also occur, but this was not detected due to the developmental stage studied. Correspondingly, mutations in the human *CASK* gene encoding another MAGUK cause both microcephaly and defects in synaptogenesis (Najm et al., 2008; Sanford et al., 2004; Atasoy et al., 2007). The trafficking of neurotransmitter receptors in adult neurons represents another level of Dlg3 function (Sans et al., 2003). The mutations identified in human *Dlg3* result in the expression of a truncated protein that, notably, contains the PY motifs and part of the PDZ domains but not the C-terminal part of the protein (Tarpey et al., 2004). This could result in the interaction of the mutated Dlg3 with Nedd4(-2) while disrupting the trafficking of the complex toward the synapse. We believe that the binding specificities of Dlg3 may play an important function for discriminating trafficking and signaling activities in the adult brain in cooperation with the E3 ligases of the Nedd4 family.

## EXPERIMENTAL PROCEDURES

### Dlg3 KO Mice, ESC Culture, and Generation of Completely ESC-Derived Embryos

The GT clone P038A02 (R1 on a pure 129Sv6 genetic background) was obtained from the German Gene Trap Consortium. *Dlg3*$^{tm1Gmt/Y}$ male and *Dlg3*$^{tm1Gmt/+}$ female mice on a C57Bl/6 background were genotyped as previously described (Cuthbert et al., 2007). ESCs were cultured on a feeder layer of mitomycin-inactivated mouse embryonic fibroblasts (MEFs) using standard protocols. Stable ESC transfectants were produced under Puromycine selection using standard protocols. Tetraploid embryos were generated by electrofusion of two-cell stage embryos isolated from ubiquitous DsRed-expressing donor females (Vintersten et al., 2004) as previously described (Nagy et al., 1993). Tetraploid embryos at three to four-cell stage were aggregated with clumps of six to eight *Dlg3*$^{P038A02/Y}$ ESCs overnight, and blastocysts were transferred into the uterus of recipients. After dissection, the contribution of tetraploid cells to the ESC-derived embryos was examined by using a Zeiss Stereo Lumar.V12 fluorescent microscope.

### Whole-Mount β-Galactosidase Staining

Embryos were fixed in PBS (pH 7.3) containing 0.02% NP-40, 5 mM EGTA, 2 mM $MgCl_2$, 1% formaldehyde, and 0.2% glutaraldehyde at room temperature for 30 min, washed briefly in PBS, and placed in X-gal staining solution (PBS containing 0.02% NP-40, 2 mM $MgCl_2$, 5 mM $K_3[Fe(CN)_6]$, 5 mM $K_4[Fe(CN)_6]$, 0.01% sodium deoxycholate, 1 mg/ml X-gal). Staining was carried out overnight at room temperature. After staining, samples were washed in PBS and stored in 4% paraformaldehyde at 4°C.

### Cryosections, Immunofluorescence, and Imaging

For cryosections, dissected embryos were fixed briefly in 4% PFA and cryoprotected by incubation in 30% sucrose. Samples were subsequently frozen in OCT medium on dry ice and stored at −20°C before being sectioned at 12 μm. Whole-mount immunofluorescence was performed as previously described (Burtscher and Lickert, 2009). The following antibodies were used: Foxa2 (Santa Cruz Biotechnology) 1:1000; T/Brachyury (Santa Cruz Biotechnology) 1:1000; E-cadherin (BD) 1:2000; ZO-1 (Invitrogen) 1:200; Arl13b (generous gift from Tamara Caspary) 1:1000; Nedd4 (Abcam) 1:500; Nedd4-2 (Cell Signaling Technology) 1:500; Flag rabbit polyclonal and M2 monoclonal (Sigma-Aldrich) 1:200; RFP (BIOTREND) 1:500; Dlg1/SAP97 (BD) 1:100; Dlg2/PSD93 (Abcam) 1:200; Dlg3/SAP102 (Abcam) 1:200; Dlg4/PSD95 (Abcam) 1:200; 58K (Sigma-Aldrich) 1:200; Rab8 (BD) 1:200; α-Tubulin (Sigma-Aldrich) 1:500; PPH3 (Millipore) 1:500; aPKC ζ (Sigma-Aldrich) 1:1000; and Phalloidin (Invitrogen) 1:50. TUNEL reactions (Roche) were performed according to the manufacturer's instructions. Immunostainings were analyzed with a Leica laser-scanning SP5 confocal microscope (20× and 63× objectives). We digitally measured colocalization using the Leica LAS-AF software based on intensity correlation analysis in two-color images. This program creates a binary image indicating colocalizing pixels above an intensity threshold.

### Statistical Analysis

Average and standard deviation are shown in the graphs in Figures 4E, S1F, S2C, S2F, S4K, S4L, and S6D. p values were determined using a chi-square test or a two-tailed Student's t test with unequal variance with the number of cells and embryos stated in the figure legends.

### IP and Immunoblotting

#### *CoIP*

Adult WT brains were lysed in TBS buffer (30 mM Tris-HCl [pH 7.4], 150 mM NaCl) supplemented with 0.5% NP-40 (Roche) and protease inhibitor cocktail (Roche). Samples were precleared with protein G Sepharose (GE Healthcare) at 4°C for 1 hr on a rotary stirrer. Protein G Sepharose beads were removed by centrifugation in a benchtop centrifuge at full speed. Equal amounts of proteins were incubated with 2 μg of Nedd4 rabbit polyclonal (Abcam) or of anti-GFP rabbit polyclonal (Invitrogen) for 1 hr at 4°C. Immunocomplexes were bound to protein G Sepharose beads overnight at 4°C, washed in lysis buffer, and analyzed by SDS-PAGE.

#### *Western Blotting*

Protein samples were separated by SDS-PAGE, and immunoblotting was performed by standard procedures. Total lysate and IP protein samples were separated on the same gel in order to check enrichment of the different proteins after IP and to compare interaction strengths. Antibodies were used in the following concentrations: Flag M2 (Sigma-Aldrich) 1:10,000; TJAP1 (Abcam) 1:1,000; pan-Nedd4 (Abcam) 1:1,000; PP1α (New England BioLabs) and Dlg3/SAP102 (Synaptic Systems) 1:3,000; GFP (Invitrogen) 1:5,000; Ubiquitin antibody (FK2; Enzo) and Myc 9E10 (Sigma-Aldrich) 1:10,000; Sec8 (BIOTREND) 1:1000; Actin (BD) 1:10,000; Nedd4 (Abcam) 1:5,000; Nedd4-2 (Cell Signaling Technology) 1:5,000; and Dynein IC (Sigma-Aldrich) 1:5,000. Protein bands were visualized using ECL detection (GE Healthcare) on Hyperfilms (GE Healthcare).

### Other Procedures

TAP and LC-MS/MS, expression vectors, whole-mount in situ hybridizations, RT-PCR, and cell culture are described in Supplemental Experimental Procedures.

## SUPPLEMENTAL INFORMATION

Supplemental Information includes six figures and Supplemental Experimental Procedures and can be found with this article online at doi:10.1016/j.devcel.2011.08.003.

## ACKNOWLEDGMENTS

We are thankful to Wenke Barkey for excellent technical assistance. We thank Tamara Caspary for the Arl13b antibody. We thank Anne Stephenson and

Morgan Sheng for MAGUK expression vectors. We thank Perry Liao and Naomi Chadderton for valuable comments on the manuscript. This work was supported by the Helmholtz Society, a European Research Council Starting Grant and an Emmy-Noether fellowship from the German Research Foundation (DFG) awarded to H.L. This work was also supported by the EU grant SYSCILIA (HEALTH-F5-2010-241955; to M.U.) and the German Federal Ministry of Education and Research (BMBF: DYNAMO, FKZ: 0315513A; to M.U.) C.A.V.C. was the recipient of an Alexander von Humboldt Foundation scholarship.

Received: May 1, 2010
Revised: May 24, 2011
Accepted: August 1, 2011
Published online: September 12, 2011

## REFERENCES

Aberle, H., Schwartz, H., and Kemler, R. (1996). Cadherin-catenin complex: protein interactions and their implications for cadherin function. J. Cell. Biochem. *61*, 514–523.

Ang, S.L., and Rossant, J. (1994). HNF-3 beta is essential for node and notochord formation in mouse development. Cell *78*, 561–574.

Aoki, C., Miko, I., Oviedo, H., Mikeladze-Dvali, T., Alexandre, L., Sweeney, N., and Bredt, D.S. (2001). Electron microscopic immunocytochemical detection of PSD-95, PSD-93, SAP-102, and SAP-97 at postsynaptic, presynaptic, and nonsynaptic sites of adult and neonatal rat visual cortex. Synapse *40*, 239–257.

Atasoy, D., Schoch, S., Ho, A., Nadasy, K.A., Liu, X., Zhang, W., Mukherjee, K., Nosyreva, E.D., Fernandez-Chacon, R., Missler, M., et al. (2007). Deletion of CASK in mice is lethal and impairs synaptic function. Proc. Natl. Acad. Sci. USA *104*, 2525–2530.

Bellaïche, Y., Radovic, A., Woods, D.F., Hough, C.D., Parmentier, M.L., O'Kane, C.J., Bryant, P.J., and Schweisguth, F. (2001). The Partner of Inscuteable/Discs-large complex is required to establish planar polarity during asymmetric cell division in *Drosophila*. Cell *106*, 355–366.

Bilder, D., Li, M., and Perrimon, N. (2000). Cooperative regulation of cell polarity and growth by *Drosophila* tumor suppressors. Science *289*, 113–116.

Bork, P., and Sudol, M. (1994). The WW domain: a signalling site in dystrophin? Trends Biochem. Sci. *19*, 531–533.

Burtscher, I., and Lickert, H. (2009). Foxa2 regulates polarity and epithelialization in the endoderm germ layer of the mouse embryo. Development *136*, 1029–1038.

Caruana, G., and Bernstein, A. (2001). Craniofacial dysmorphogenesis including cleft palate in mice with an insertional mutation in the discs large gene. Mol. Cell. Biol. *21*, 1475–1483.

Caspary, T., Larkins, C.E., and Anderson, K.V. (2007). The graded response to Sonic Hedgehog depends on cilia architecture. Dev. Cell *12*, 767–778.

Cox, B.J., Vollmer, M., Tamplin, O., Lu, M., Biechele, S., Gertsenstein, M., van Campenhout, C., Floss, T., Kühn, R., Wurst, W., et al. (2010). Phenotypic annotation of the mouse X chromosome. Genome Res. *20*, 1154–1164.

Cuthbert, P.C., Stanford, L.E., Coba, M.P., Ainge, J.A., Fink, A.E., Opazo, P., Delgado, J.Y., Komiyama, N.H., O'Dell, T.J., and Grant, S.G. (2007). Synapse-associated protein 102/dlgh3 couples the NMDA receptor to specific plasticity pathways and learning strategies. J. Neurosci. *27*, 2673–2682.

Egea, J., Erlacher, C., Montanez, E., Burtscher, I., Yamagishi, S., Hess, M., Hampel, F., Sanchez, R., Rodriguez-Manzaneque, M.T., Bösl, M.R., et al. (2008). Genetic ablation of FLRT3 reveals a novel morphogenetic function for the anterior visceral endoderm in suppressing mesoderm differentiation. Genes Dev. *22*, 3349–3362.

Fotia, A.B., Cook, D.I., and Kumar, S. (2006). The ubiquitin-protein ligases Nedd4 and Nedd4-2 show similar ubiquitin-conjugating enzyme specificities. Int. J. Biochem. Cell Biol. *38*, 472–479.

Gloeckner, C.J., Boldt, K., Schumacher, A., Roepman, R., and Ueffing, M. (2007). A novel tandem affinity purification strategy for the efficient isolation and characterisation of native protein complexes. Proteomics *7*, 4228–4234.

Hashimoto, M., Shinohara, K., Wang, J., Ikeuchi, S., Yoshiba, S., Meno, C., Nonaka, S., Takada, S., Hatta, K., Wynshaw-Boris, A., and Hamada, H. (2010). Planar polarization of node cells determines the rotational axis of node cilia. Nat. Cell Biol. *12*, 170–176.

Hendrickx, A., Beullens, M., Ceulemans, H., Den Abt, T., Van Eynde, A., Nicolaescu, E., Lesage, B., and Bollen, M. (2009). Docking motif-guided mapping of the interactome of protein phosphatase-1. Chem. Biol. *16*, 365–371.

Hsu, S.C., Hazuka, C.D., Foletti, D.L., and Scheller, R.H. (1999). Targeting vesicles to specific sites on the plasma membrane: the role of the sec6/8 complex. Trends Cell Biol. *9*, 150–153.

Huibregtse, J.M., Scheffner, M., Beaudenon, S., and Howley, P.M. (1995). A family of proteins structurally and functionally related to the E6-AP ubiquitin-protein ligase. Proc. Natl. Acad. Sci. USA *92*, 2563–2567.

Izumi, Y., Hirose, T., Tamai, Y., Hirai, S., Nagashima, Y., Fujimoto, T., Tabuse, Y., Kemphues, K.J., and Ohno, S. (1998). An atypical PKC directly associates and colocalizes at the epithelial tight junction with ASIP, a mammalian homologue of *Caenorhabditis elegans* polarity protein PAR-3. J. Cell Biol. *143*, 95–106.

Kanelis, V., Rotin, D., and Forman-Kay, J.D. (2001). Solution structure of a Nedd4 WW domain-ENaC peptide complex. Nat. Struct. Biol. *8*, 407–412.

Kanelis, V., Bruce, M.C., Skrynnikov, N.R., Rotin, D., and Forman-Kay, J.D. (2006). Structural determinants for high-affinity binding in a Nedd4 WW3* domain-Comm PY motif complex. Structure *14*, 543–553.

Katsuno, T., Umeda, K., Matsui, T., Hata, M., Tamura, A., Itoh, M., Takeuchi, K., Fujimori, T., Nabeshima, Y., Noda, T., et al. (2008). Deficiency of zonula occludens-1 causes embryonic lethal phenotype associated with defected yolk sac angiogenesis and apoptosis of embryonic cells. Mol. Biol. Cell *19*, 2465–2475.

Kawabe, H., Nakanishi, H., Asada, M., Fukuhara, A., Morimoto, K., Takeuchi, M., and Takai, Y. (2001). Pilt, a novel peripheral membrane protein at tight junctions in epithelial cells. J. Biol. Chem. *276*, 48350–48355.

Kinder, S.J., Tsang, T.E., Wakamiya, M., Sasaki, H., Behringer, R.R., Nagy, A., and Tam, P.P. (2001). The organizer of the mouse gastrula is composed of a dynamic population of progenitor cells for the axial mesoderm. Development *128*, 3623–3634.

Klezovitch, O., Fernandez, T.E., Tapscott, S.J., and Vasioukhin, V. (2004). Loss of cell polarity causes severe brain dysplasia in Lgl1 knockout mice. Genes Dev. *18*, 559–571.

Kwon, G.S., Viotti, M., and Hadjantonakis, A.K. (2008). The endoderm of the mouse embryo arises by dynamic widespread intercalation of embryonic and extraembryonic lineages. Dev. Cell *15*, 509–520.

Lafont, F., Burkhardt, J.K., and Simons, K. (1994). Involvement of microtubule motors in basolateral and apical transport in kidney cells. Nature *372*, 801–803.

Lemmers, C., Michel, D., Lane-Guermonprez, L., Delgrossi, M.H., Médina, E., Arsanto, J.P., and Le Bivic, A. (2004). CRB3 binds directly to Par6 and regulates the morphogenesis of the tight junctions in mammalian epithelial cells. Mol. Biol. Cell *15*, 1324–1333.

Mahoney, Z.X., Sammut, B., Xavier, R.J., Cunningham, J., Go, G., Brim, K.L., Stappenbeck, T.S., Miner, J.H., and Swat, W. (2006). Discs-large homolog 1 regulates smooth muscle orientation in the mouse ureter. Proc. Natl. Acad. Sci. USA *103*, 19872–19877.

Matern, H.T., Yeaman, C., Nelson, W.J., and Scheller, R.H. (2001). The Sec6/8 complex in mammalian cells: characterization of mammalian Sec3, subunit interactions, and expression of subunits in polarized cells. Proc. Natl. Acad. Sci. USA *98*, 9648–9653.

Migaud, M., Charlesworth, P., Dempster, M., Webster, L.C., Watabe, A.M., Makhinson, M., He, Y., Ramsay, M.F., Morris, R.G., Morrison, J.H., et al. (1998). Enhanced long-term potentiation and impaired learning in mice with mutant postsynaptic density-95 protein. Nature *396*, 433–439.

Montcouquiol, M., Rachel, R.A., Lanford, P.J., Copeland, N.G., Jenkins, N.A., and Kelley, M.W. (2003). Identification of Vangl2 and Scrb1 as planar polarity genes in mammals. Nature *423*, 173–177.

Murillas, R., Simms, K.S., Hatakeyama, S., Weissman, A.M., and Kuehn, M.R. (2002). Identification of developmentally expressed proteins that functionally interact with Nedd4 ubiquitin ligase. J. Biol. Chem. *277*, 2897–2907.

Nagy, A., Rossant, J., Nagy, R., Abramow-Newerly, W., and Roder, J.C. (1993). Derivation of completely cell culture-derived mice from early-passage embryonic stem cells. Proc. Natl. Acad. Sci. USA *90*, 8424–8428.

Naim, E., Bernstein, A., Bertram, J.F., and Caruana, G. (2005). Mutagenesis of the epithelial polarity gene, discs large 1, perturbs nephrogenesis in the developing mouse kidney. Kidney Int. *68*, 955–965.

Najm, J., Horn, D., Wimplinger, I., Golden, J.A., Chizhikov, V.V., Sudi, J., Christian, S.L., Ullmann, R., Kuechler, A., Haas, C.A., et al. (2008). Mutations of CASK cause an X-linked brain malformation phenotype with microcephaly and hypoplasia of the brainstem and cerebellum. Nat. Genet. *40*, 1065–1067.

Narimatsu, M., Bose, R., Pye, M., Zhang, L., Miller, B., Ching, P., Sakuma, R., Luga, V., Roncari, L., Attisano, L., and Wrana, J.L. (2009). Regulation of planar cell polarity by Smurf ubiquitin ligases. Cell *137*, 295–307.

Ohno, S. (2001). Intercellular junctions and cellular polarity: the PAR-aPKC complex, a conserved core cassette playing fundamental roles in cell polarity. Curr. Opin. Cell Biol. *13*, 641–648.

Plant, P.J., Lafont, F., Lecat, S., Verkade, P., Simons, K., and Rotin, D. (2000). Apical membrane targeting of Nedd4 is mediated by an association of its C2 domain with annexin XIIIb. J. Cell Biol. *149*, 1473–1484.

Roh, M.H., Fan, S., Liu, C.J., and Margolis, B. (2003). The Crumbs3-Pals1 complex participates in the establishment of polarity in mammalian epithelial cells. J. Cell Sci. *116*, 2895–2906.

Sanford, J.L., Mays, T.A., and Rafael-Fortney, J.A. (2004). CASK and Dlg form a PDZ protein complex at the mammalian neuromuscular junction. Muscle Nerve *30*, 164–171.

Sans, N., Prybylowski, K., Petralia, R.S., Chang, K., Wang, Y.X., Racca, C., Vicini, S., and Wenthold, R.J. (2003). NMDA receptor trafficking through an interaction between PDZ proteins and the exocyst complex. Nat. Cell Biol. *5*, 520–530.

Shin, K., Fogg, V.C., and Margolis, B. (2006). Tight junctions and cell polarity. Annu. Rev. Cell Dev. Biol. *22*, 207–235.

Staub, O., Dho, S., Henry, P., Correa, J., Ishikawa, T., McGlade, J., and Rotin, D. (1996). WW domains of Nedd4 bind to the proline-rich PY motifs in the epithelial Na+ channel deleted in Liddle's syndrome. EMBO J. *15*, 2371–2380.

Suzuki, A., Yamanaka, T., Hirose, T., Manabe, N., Mizuno, K., Shimizu, M., Akimoto, K., Izumi, Y., Ohnishi, T., and Ohno, S. (2001). Atypical protein kinase C is involved in the evolutionarily conserved par protein complex and plays a critical role in establishing epithelia-specific junctional structures. J. Cell Biol. *152*, 1183–1196.

Tam, P.P., and Rossant, J. (2003). Mouse embryonic chimeras: tools for studying mammalian development. Development *130*, 6155–6163.

Tanentzapf, G., and Tepass, U. (2003). Interactions between the crumbs, lethal giant larvae and bazooka pathways in epithelial polarization. Nat. Cell Biol. *5*, 46–52.

Tarpey, P., Parnau, J., Blow, M., Woffendin, H., Bignell, G., Cox, C., Cox, J., Davies, H., Edkins, S., Holden, S., et al. (2004). Mutations in the DLG3 gene cause nonsyndromic X-linked mental retardation. Am. J. Hum. Genet. *75*, 318–324.

Tepass, U. (2003). Claudin complexities at the apical junctional complex. Nat. Cell Biol. *5*, 595–597.

Tepass, U., Theres, C., and Knust, E. (1990). crumbs encodes an EGF-like protein expressed on apical membranes of *Drosophila* epithelial cells and required for organization of epithelia. Cell *61*, 787–799.

Traweger, A., Wiggin, G., Taylor, L., Tate, S.A., Metalnikov, P., and Pawson, T. (2008). Protein phosphatase 1 regulates the phosphorylation state of the polarity scaffold Par-3. Proc. Natl. Acad. Sci. USA *105*, 10402–10407.

Vintersten, K., Monetti, C., Gertsenstein, M., Zhang, P., Laszlo, L., Biechele, S., and Nagy, A. (2004). Mouse in red: red fluorescent protein expression in mouse ES cells, embryos, and adult animals. Genesis *40*, 241–246.

Woods, D.F., Hough, C., Peel, D., Callaini, G., and Bryant, P.J. (1996). Dlg protein is required for junction structure, cell polarity, and proliferation control in *Drosophila* epithelia. J. Cell Biol. *134*, 1469–1482.

Yeaman, C., Grindstaff, K.K., and Nelson, W.J. (2004). Mechanism of recruiting Sec6/8 (exocyst) complex to the apical junctional complex during polarization of epithelial cells. J. Cell Sci. *117*, 559–570.